Electronic Spectrum of the .alpha.,.alpha.-Difluoroethyl Radical

ARTICLE *in* THE JOURNAL OF PHYSICAL CHEMISTRY · MAY 2002

Impact Factor: 2.78 · DOI: 10.1021/j100065a017

3 AUTHORS:

Jeffrey Brum

GlaxoSmithKline plc.

34 PUBLICATIONS **351** CITATIONS

SEE PROFILE

Russell Johnson

National Institute of Standards and Technology

77 PUBLICATIONS **1,271** CITATIONS

SEE PROFILE

Jeffrey W Hudgens

National Institute of Standards and Technology

135 PUBLICATIONS **2,249** CITATIONS

SEE PROFILE

Electronic Spectrum of the α,α-Difluoroethyl Radical

Jeffrey L. Brum,† Russell D. Johnson, III,* and Jeffrey W. Hudgens*

Chemical Kinetics and Thermodynamics Division, Chemical Science and Technology Laboratory, National Institute of Standards and Technology,‡ Gaithersburg, Maryland 20899

Received: December 1, 1993; In Final Form: January 28, 1994•

The first electronic spectrum of the α,α-difluoroethyl radical (CF_2CH_3) was observed between 335 and 475 nm by resonance-enhanced multiphoton ionization (REMPI) spectroscopy. The spectrum arises from two-photon resonances with a 3p Rydberg state. A third laser photon ionized the radicals. The electronic origin is tentatively assigned at ν_{00} = 43 275 cm^{-1}, and the vibrational progression is assigned as the $\nu_9'(CF_2$ wag) = 530 cm^{-1}. In support of these spectral assignments, we report *ab initio* calculations at the MP2/6-31G*, G1, and G2 theory levels which found the optimum structures, vibrational frequencies, and relative energies of CF_2CH_3, $CF_2CH_3^+$, CHF_2CH_2, and $CHF_2CH_2^+$.

Introduction

The link between anthropogenic chlorofluorocarbon (CFC) release and stratospheric ozone depletion now appears well established. Several fluorinated ethanes are among the hydrofluorocarbons (HFCs) currently being investigated as replacements for the chlorine-containing congeners that have traditionally found use as refrigerants and fire extinguishers and in more specialized applications. In recent years, significant effort has focused on the tropospheric degradation pathways available to HFCs initiated by H atom abstraction by a hydroxyl radical. For fluorinated ethanes the generic initiating reactions are

$$C_2H_{6-x}F_x + OH \rightarrow C_2H_{6-x-1}F_x + H_2O \qquad (1)$$

Although an impressive amount of mechanistic and kinetic information concerning these pathways has been gathered recently,[1] much remains to be learned about the fluorinated ethyl radicals which represent the first intermediate of the degradation process.

In this regard we have investigated the radicals produced by H atom abstraction from 1,1-difluoroethane (HFC 152a) using resonance-enhanced multiphoton ionization (REMPI) spectroscopy. We report the first electronic spectrum of the CF_2CH_3 radical. This spectrum also represents the first observation of a vibrationally resolved electronic excited state of a substituted ethyl radical. Specifically, the system is investigated between 335 and 475 nm with vibronic structure observed between 420 and 462 nm. The results of *ab initio* calculations of the $C_2H_3F_2$ radicals and cations aided the spectral assignments.

Experimental and Computational Methods

The experimental apparatus used in these studies consisted of a tunable dye laser, flow reactor, time-of-flight mass spectrometer, and computerized data acquisition system. The apparatus is described in detail elsewhere.[2] In a flow reactor (pressure = 200–400 Pa, flow rate = 1–3 m/s) fluorine atoms were reacted with CHF_2CH_3 (HFC 152a, PCR Inc.),[3] which produced radicals via

$$CHF_2CH_3 + F \rightarrow CHF_2CH_2 + HF \qquad (2a)$$

$$\rightarrow CF_2CH_3 + HF \qquad (2b)$$

Atomic fluorine was produced by passing mixtures comprised of <1% fluorine and >99% helium through a microwave discharge. The radicals effused from the reactor into the ionization region of a time-of-flight mass spectrometer where they were exposed to the focused output of an excimer-pumped dye laser (Lambda Physik EMG 201MSC and Lambda Physik FL 2002).[3] The mass-analyzed signal was collected and averaged by a computerized data acquisition system.

Calculations of $C_2H_3F_2$ species were performed using the Gaussian 92 series of programs[4] on CRAY Y-MP and Convex C3820 computers located at NIST. Using the 6-31G* basis set, optimized geometries and vibrational frequencies were calculated for all CF_2CH_3 and CHF_2CH_2 species at the unrestricted Hartree–Fock (UHF) level. To find the lowest-energy structure of each species, geometry optimizations were performed starting with various torsional angles. The lowest-energy structures found by the UHF calculations were reoptimized by adding electron correlation effects via Møller–Plesset perturbation theory carried to second order (MP2/6-31G*). Finally, while holding the geometry of each species to its MP2/6-31G* structure, we calculated total energies at higher levels of electron correlation and basis set. Following the prescriptions of Pople et al.,[5] we combined higher-level results to obtain the total energies at the G1 and G2 levels.

Results

***Ab Initio* Calculations.** This study examined the ion signals appearing between 480 and 335 nm. Prior experience has established that within this wavelength region halomethyl radicals produce REMPI spectra via two-photon resonances with their Rydberg states.[6-9] We expect the haloethyl radicals to behave similarly. To assist with the interpretation of the REMPI spectra, we performed *ab initio* calculations on difluoroethyl radicals and cations to determine their geometries, vibrational frequencies, and the ionization potentials. We calculate properties of cations and use them to approximate those of Rydberg radicals. This simplification works because Rydberg states have the same core electron configuration as the cation. Thus, the structure and vibrational frequencies of the cation closely approximate those of the Rydberg states. Previous studies have found that this strategy reliably predicts the vibrational frequencies observed in REMPI spectra.[10-13]

* Address correspondence to these authors.
† NIST/NRC Postdoctoral Associate.
‡ Formerly called the National Bureau of Standards.
• Abstract published in *Advance ACS Abstracts*, March 1, 1994.

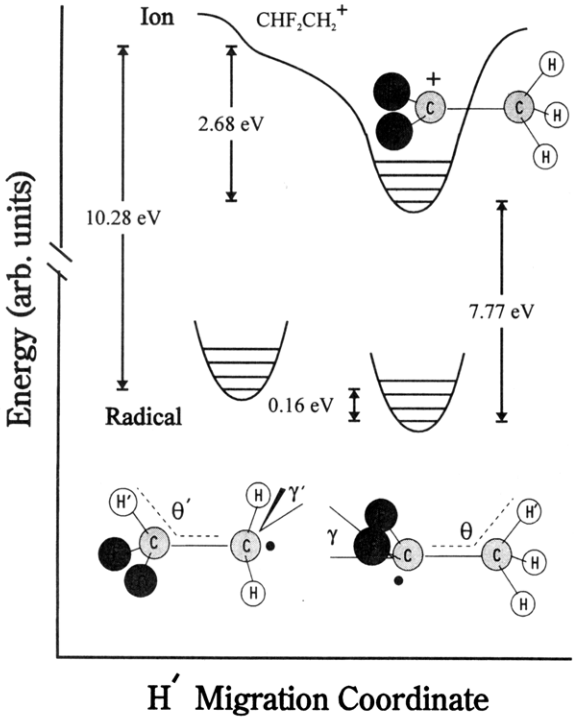

Figure 1. Atom labeling, geometric parameters, and energy level diagram for CF_2CH_3 and CHF_2CH_2 species. Energies are obtained from the *ab initio* results at the G1 theory level. See text.

Figure 1 illustrates the atom labeling and bond angles of CF_2CH_3 and CHF_2CH_2. Table 1 lists the total energies, optimized geometries, and ionization potentials of CF_2CH_3 and CHF_2CH_2 radicals and cations. At the MP2/6-31G* and higher levels of theory the *ab initio* calculations predict stable structures for CF_2CH_3, $CF_2CH_3^+$, and CHF_2CH_2. Although UHF/6-31G* level geometry optimizations of $CHF_2CH_2^+$ converge to a stable structure, optimizations at the MP2/6-31G* level and higher predict that $CHF_2CH_2^+$ is a nonstationary structure that isomerizes to form either $CHFCH_2F^+$ or $CF_2CH_3^+$, depending upon the $CHF_2CH_2^+$ rotamer at the start of each calculation. The lowest-energy cation structure is $CF_2CH_3^+$.[14] In $CHFCH_2F^+$ and $CF_2CH_3^+$ a halogen atom on the sp^2-bonded carbocation center helps stabilize the structure. In a separate *ab initio* study we explored the stability of several halogenated ethyl cations. In each case we found that the lowest-energy structure is one which has a carboncation site stabilized by halogen atoms.[15]

The *ab initio* G1 method predicts 7.77 eV, and the G2 method predicts $IP_a(CF_2CH_3) = 7.76$ eV (Table 1). These values agree reasonably well with the experimental value, $IP_a(CF_2CH_3) = 7.62$ eV, obtained from the enthalpies of formation, $\Delta H_f°_0(CF_2CH_3)$[16] and $\Delta H_f°_0(CF_2CH_3^+)$.[17]

Figure 1 displays the energy relationships among the radicals and cations derived from *ab initio* calculations at the G1 level. The CF_2CH_3 radical has the lowest-energy structure, and the CHF_2CH_2 radical lies 0.13 eV above it. The stable $CF_2CH_3^+$ structure resides $IP_a(CF_2CH_3) = 7.77$ eV above the CF_2CH_3 radical. Because $CHF_2CH_2^+$ isomerizes to $CF_2CH_3^+$, the adiabatic ionization potential of the CHF_2CH_2 radical is referenced to $CF_2CH_3^+$, which gives $IP_a(CHF_2CH_2) = 7.60$ eV. We obtained the vertical ionization potential, $IP_v(CHF_2CH_2) = 10.28$ eV, by calculating a single point on the ion potential surface at the neutral CHF_2CH_2 equilibrium geometry. This procedure estimates that the $CHF_2CH_2^+$ nonstationary structure resides ~2.68 eV above the $CF_2CH_3^+$ isomer.

Table 2 lists the scaled vibrational frequencies calculated at the UHF/6-31G* level at the UHF minimum structure. These frequencies were obtained by reducing the GAUSSIAN results by 11% so that the systematic error known to accompany UHF frequency calculations is minimized.[18] These scaled HF/6-31G* frequencies provide the zero point energy (ZPE) corrections which we used in higher-level calculations. In agreement with the finding that $CHF_2CH_2^+$ is a nonstationary structure, *ab initio* calculations of $CHF_2CH_2^+$ at the MP2/6-31G* level always produced one imaginary vibrational frequency.

Using the *ab initio* results, we can estimate the vibrational activity of Rydberg spectra produced from CF_2CH_3. When CF_2CH_3 is excited vertically into a Rydberg state, a $CF_2CH_3^+$ core is formed that closely resembles the cation ground state. The geometry differences between the radical and the cation govern which vibrational modes are active. By treating the radical and cation as classical uncoupled oscillators, we have estimated the median number of quanta in each cation mode by projecting mass-weighted geometry differences onto the cation normal vibrational modes via eqs 3a and 3b:

$$E_{vert}(n) = \frac{50341k_n}{2\mu_n^2}\left(\sum_i m_i v_{i,n}(q_i - q_i^+)\right)^2 \qquad (3a)$$

$$\text{quanta}(n) = E_{vert}(n)/\omega_n \qquad (3b)$$

where q_i and q_i^+ are the atomic coordinates (Å), $v_{i,n}$ are the normal coordinates expressed in Cartesian coordinates for a given vibrational mode n, μ_n is the reduced mass (amu) of the nth vibrational mode, m_i is the mass (amu) of the ith coordinate ($m_1 = 12$, $m_2 = 12$, $m_3 = 12$, $m_4 = 19$, ...), k_n is the force constant (mdyn/Å) of vibrational mode n, $E_{vert}(n)$ is the classical energy (cm^{-1}) contained in mode n, and ω_n is the vibrational frequency (cm^{-1}) of mode n. MP2/6-31G* calculations of the ion and neutral provided the Cartesian coordinates of the atoms, Cartesian coordinates for the normal modes, and the force constants and frequencies. During the calculation of $E_{vert}(n)$ we aligned the center of masses and principal rotational axes to eliminate contamination by rotation.

We emphasize that eq 3a represents a classical approximation in which we estimate the amount of energy available for vibrational excitation for each uncoupled mode by the coordinate displacement (neutral – ion) within the appropriate harmonic oscillator of the cation. The conversion to number of quanta excited is the final step (eq 3b), and due to the classical nature of eq 3a we obtain noninteger values from eq 3b. When unscaled vibrational frequencies are used to calculate $E_{vert}(n)$, the total vibrational energy, $\sum E_{vert}(n)$, should correspond to the difference, $IP_v(CF_2CH_3) - IP_a(CF_2CH_3)$. At the MP2/6-31G* level we obtain $\sum E_{vert}(n) = 1.48$ eV and $IP_v(CF_2CH_3) - IP_a(CF_2CH_3) = 1.52$ eV (Tables 1 and 2). This good agreement helps validate the computations obtained with eq 3.

Table 2 lists the median number of quanta within each vibrational mode of the $CF_2CH_3^+$ core predicted to appear in Rydberg spectra. Equation 3 predicts that Rydberg spectra will show a median excitation of 8.3 quanta in the CF_2 out-of-plane wag ($\nu_9 = 521$ cm^{-1}) and 4.4 quanta in the CH_3 rocking mode ($\nu_6 = 1038$ cm^{-1}). The large geometry change from $\gamma = 44.2°$ in the radical to $\gamma \sim 0°$ in the cation activates these vibrational modes, where γ is the angle formed between the plane of the CF_2 group and the C–C bond. Therefore, REMPI spectra of Rydberg states should show progressions along the ν_6 and ν_9 modes.

The *ab initio* results also enable predictions about the appearance of Rydberg spectra produced from CHF_2CH_2. When CHF_2CH_2 is excited into a Rydberg state, the newly formed $CHF_2CH_2^+$ core rapidly rearranges into a vibrationally excited $CF_2CH_3^+$ core. For each Rydberg state the large density of vibrational states at the energy of the unstable $CHF_2CH_2^+$ core form a continuum. Near the lower-energy, stable $CF_2CH_3^+$ core, the absorption strength will vanish. Therefore, the absorption maxima of Rydberg states of CHF_2CH_2 radicals are displaced substantially to higher energy relative to their electronic origins.

TABLE 1: *Ab Initio* Geometries, Total Energies, and Ionization Potentials Calculated for the Ground Electronic States of CF_2CH_3 and CHF_2CH_2 Radicals and Cations[a]

parameter	CF_2CH_3 C_s	$CF_2CH_3^+$ C_s	CHF_2CH_2 C_1	$CHF_2CH_2^+$ [b]
γ, deg[c]	44.2	1.6		
γ′, deg[d]			13.9	
θ(C–C–H′), deg	109.76	106.44		
θ′(H′–C–C), deg			113.91	
r(C–F), Å	1.347	1.260	1.371, 1.381[e]	
r(C–C), Å	1.487	1.450	1.477	
r(C–H), Å	1.095	1.104		
r(C–H′), Å			1.093	
MP2/6-31G* energy (optimized geometry), hartrees[f]	−276.9018277	−276.6351287	−276.8923633	
MP2/6-31G* (radical geometry), hartrees[f]		−276.5790225		−276.5288649
MP2 IP_v, eV	8.78		9.89	
MP2 IP_a, eV	7.26		7.0[g]	
MP4/6-311G** energy, hartrees[f]	−277.1069848	−276.8348365	−277.0991005	−276.7287673
MP4/6-311+G* energy, hartrees[f]	−277.121738	−276.8415639	−277.1150517	−276.7399897
MP4/6-311G** (2df) energy, hartrees[f]	−277.2488936	−276.9753615	−277.2404385	−276.867958
QCISD(T)/6-311G** energy, hartrees[f]	−277.1060615	−276.831123	−277.098155	−276.7280012
G1 energy, hartrees[f]	−277.2912640	−277.0058608	−277.2852731	−276.9074284
G1 IP_v, eV			10.28	
G1 IP_a, eV	7.77		7.60[g]	
MP2/6-311G(d,p) energy, hartrees[f]	−277.0614211	−276.7892219		
MP2/6-311+G(d,p) energy, hartrees[f]	−277.075046	276.795144		
MP2/6-311G(2df,p) energy, hartrees[f]	−277.1964569	−276.9238119		
MP2/6-311+G(3df,2p) energy, hartrees,[f]	−277.2272205	−276.9469172		
G2 energy, hartrees[f]	−277.2947227	−277.0093640		
G2 IP_a, eV	7.76			

[a] Unless noted otherwise, values shown are calculated at the MP2/6-31G* level of theory. Figure 1 shows the atom labeling and geometric parameters. [b] This isomer is not stable. The energy was obtained from a single-point calculation at the equilibrium geometry of the neutral for a reference point on the excited-state surface, approximating a vertical IP. From this particular geometry, 1,2H atom migration proceeds to the $CF_2CH_3^+$ minimum. See text. [c] γ is the angle formed between the CF_2 plane and the C–C bond. [d] γ′ is the angle formed between the CH_2 plane and the C–C bond. [e] C_1 symmetry results in the C–F bonds not being equivalent. [f] 1 hartree = 219 474 cm^{-1}. [g] $IP_a(CHF_2CH_2)$ is referenced to the $CF_2CH_3^+$. See text.

We estimate that the continuous absorption band associated with each Rydberg transition of CHF_2CH_2 will appear about 2.51 eV higher in energy than the corresponding origin band observed from CF_2CH_3.

Although valence and Rydberg excited states may also be investigated using some commonly available *ab initio* methods, computed excitation energies are generally not accurate enough to fully confirm or refute our Rydberg assignment.

Experimental Data and Analysis. Difluoroethyl radicals, CF_2CH_3 and CHF_2CH_2, were generated via reaction 2. The branching ratio of reaction 2 is unknown. Figure 2 shows the m/z 65 REMPI spectrum which appears between 415 and 470 nm. Figure 2 is a composite spectrum assembled from spectra obtained with several laser dyes. To minimize distortions associated with changes in dye energy, the contribution of each dye to Figure 2 is restricted to the interval over which the dye laser energy changes slowly.

The intensity of the m/z 65 REMPI signal was proportional to the concentration of F_2 and 1,1-difluoroethane ($C_2H_4F_2$). REMPI signals ceased when the microwave discharge used to produce F atoms was extinguished. Thus, the evidence supports an assignment of the REMPI spectra to $C_2H_3F_2$ radicals. Since the REMPI spectra are carried only by the molecular ion, $C_2H_3F_2^+$, we conclude that $C_2H_3F_2^+$ does not photofragment when exposed to intense laser light between 452 and 335 nm.

Secondary reactions produced other radicals. Between 335 and 480 nm the flow reactor effluent displayed optical and mass REMPI spectra that confirmed the presence of CH_2F (m/z 33),[7] CHF_2 (m/z 51),[11] and CF (m/z 31). A plausible source of these radicals is the secondary reaction sequence:

$$CHF_2CH_2 + F \rightarrow CHF_2 + CH_2F \quad (4a)$$

$$CH_2F + 2F \rightarrow HCF + F + HF \rightarrow CF + 2HF \quad (4b)$$

In the m/z 65 REMPI spectrum the onset of ion signal lies near 462 nm, and the signal intensifies at shorter laser wavelengths. Table 3 lists all distinct vibrational bands and their energies. In Figure 2 festoons mark the vibrational progression that contains six members. Other bands which are not part of this progression lie at 421.6, 431.3, and 436.7 nm. Starting near 420 nm and continuing into the blue, the spectrum becomes structureless and shows only broad diffuse features.

The data and *ab initio* calculations support the assignment of this REMPI spectrum to two photon resonances with a 3p Rydberg state of the CF_2CH_3 radical. When we assume two-photon transitions prepare the upper state, the vibrational frequency of progression is $2h\nu \sim 530$ cm^{-1}. This vibrational frequency matches the *ab initio* value of the ν_9(CF_2 wag) mode of $CF_2CH_3^+$ and the six REMPI bands that comprise the progression approximate the activity predicted for the ν_9'(CF_2 wag) mode (Table 2). On these bases we assign the REMPI spectrum to a Rydberg state of the CF_2CH_3 radical. *Ab initio* calculations also predict that the ν_6'(CH_3 rock) mode of CF_2CH_3 may contribute to the Rydberg spectrum. However, because its predicted frequency, $\nu_6' = 1038$ cm^{-1}, is nearly a harmonic of the ν_9'(CF_2

TABLE 2: Vibrational Frequencies of the Stable CF_2CH_3 and CHF_2CH_2 Radicals and Cations[a]

	CF_2CH_3		$CF_2CH_3^+$			CHF_2CH_2	
mode no.	mode description[b]	freq, cm^{-1}	mode description[b]	freq, cm^{-1}	calc vib excitation, quanta	mode description[c]	freq, cm^{-1}
1	a' CH_3 d-stretch	2926	a' CH_3 d-stretch	2930	0	CH_2 a-str	3076
2	a' CH_3 s-stretch	2853	a' CH_3 s-stretch	2822	0	CH_2 s-str	2975
3	a' CH_3 d-deform	1442	a' CF_2 sym str	1474	0.1	CF_2-H str	2954
4	a' CH_3 s-deform	1403	a' CH_3 s-deform	1399	0.2	CH_2 sciss	1436
5	a' CF_2 sym str	1246	a' CH_3 d-deform	1351	0.3	CCH deform	1381
6	a' CH_3 rock	1077	a' CH_3 rock	1038	4.4	CCH deform	1362
7	a' CC str	834	a' CC str	834	1.1	CF_2 str	1144
8	a' CF_2 sciss	518	a' CF_2 sciss	565	0.8	CC str	1109
9	a' CF_2 wag	442	a' CF_2 wag	521	8.3	CF_2 a-str	1051
10	a'' CH_3 d-stretch	2956	a'' CH_3 d-stretch	2989	0	CF_2 str	860
11	a'' CH_3 twist	1445	a'' CF_2 a-stretch	1557	0	deform	588
12	a'' CF_2 a-stretch	1245	a'' CH_3 twist	1362	0	CH_2 wag	502
13	a'' CH_3 rock	970	a'' CH_3 rock	1012	0	CH_2 rock	439
14	a'' CF_2 twist	353	a'' CF_2 twist	389	0	CH_2 wag	333
15	a'' torsion	186	a'' torsion	41	0	torsion	125
	zero-point energy $\sum E_{vert}(n)$, eV	9948		10142	1.48[d]		9668

[a] *Ab initio* frequencies of harmonic vibrational modes were calculated at the HF/6-31G* level of theory and reduced by 11%. [b] C_s symmetry. [c] C_1 symmetry. All vibrations have A symmetry. [d] Calculated using MP2/6-31+G* geometries and frequencies.

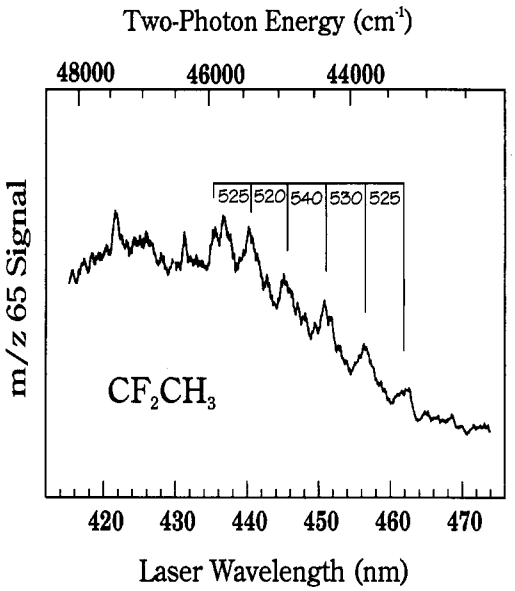

Figure 2. Composite m/z 65 REMPI spectrum of the CF_2CH_3 radical observed between 415 and 475 nm.

TABLE 3: Observed m/z 65 REMPI Bands Assigned to a 3p Rydberg State of the CF_2CH_3 Radical

λ_{laser}, nm	two-photon energy (vac), cm^{-1}	relative energy, cm^{-1}	assignment[a]
462.0	43 275 ± 40	0	0_0^0 or 9_0^n
456.5	43 800 ± 40	525	9_0^{1+n}
451.0	44 330 ± 40	1055	9_0^{2+n}
445.6	44 870 ± 35	1595	9_0^{3+n}
440.5	45 390 ± 30	2115	9_0^{4+n}
436.7	45 780 ± 30	2505	
435.5	45 915 ± 30	2640	9_0^{5+n}
431.3	46 355 ± 30	3060	
421.6	47 430 ± 30	4155	

[a] n = 0, 1, 2, 3, ...

wag) mode, its bands may blend with members of $\nu_9'(CF_2$ wag) progression. Thus, we cannot resolve the contributions by the ν_6' mode to the REMPI spectrum. A Rydberg state assignment also defines the REMPI mechanism. After absorbing one more laser photon, the 3p Rydberg radicals ionize; i.e., ion signal appears via a 2 + 1 REMPI mechanism.

We determine the character of the Rydberg orbital by solving the Rydberg equation

$$\nu_{00}\ (cm^{-1}) = IP_a(CF_2CH_3) - 109737/(n-\delta)^2 \qquad (5)$$

where n is the principal quantum number and δ is the quantum defect. When we adopt the terminus of the ν_9' progression at 462.0 nm as the electronic origin (ν_{00} = 43 275 cm^{-1}), the Rydberg equation yields the solution n = 3 and δ = 0.62, which is reasonable. Since previous studies of methyl and halomethyl radicals have found that the quantum defects of the np Rydberg series are in the range δ = 0.38–0.66,[6,19-23] these solutions establish that the REMPI spectrum arises from a 3p Rydberg state of CF_2CH_3.

The alternate assignment of the REMPI spectrum to a 3s Rydberg state (δ = 1.0) is unreasonable. Such an assignment would imply that the electronic origin lies 18 $\nu_9'(CF_2$ wag) quanta below the 462.0-nm band. Because the REMPI spectrum shows no confirmatory hot band structure, our designation of the 462.0-nm band as the origin is tentative. Since the six bands of $\nu_9'(CF_2$ wag) progression approximate the amount of predicted activity, we believe that the assignment error is small. We estimate that the actual origin resides no more than three $\nu_9'(CF_2$ wag) quanta below the 462.0-nm band (ν = 41 500 cm^{-1}). Within this limit of uncertainty, the the Rydberg equation produces quantum defects that support a 3p Rydberg assignment. In Table 3 the band designations acknowledge the possible alternate vibrational assignments.

We attribute the m/z 65 REMPI continuum spectrum between 460 and 335 nm to overlapping bands originating from vibrational levels of CF_2CH_3. Starting near 412 nm and continuing to the blue, one or more 3d Rydberg states ($\delta \sim 0.1$) may also contribute to the congested spectrum.

We cannot dismiss the possibility that the CHF_2CH_2 radical contributes to the REMPI spectrum between 360 and 335 nm. If the CHF_2CH_2 radical does contribute in this region, the m/z 65 signal should originate from two-photon resonances with higher-lying vibrational levels of the 3s Rydberg state. Because the Rydberg states of CHF_2CH_2 rapidly isomerize into the CF_2-CH_3 structure, this REMPI spectrum of CHF_2CH_2 radicals should appear as a featureless continuum.

Discussion

The properties and REMPI spectrum of CF_2CH_3 are analogous to those of CHF_2, which was studied previously.[11] In both systems *ab initio* calculations show that the geometry around the

substituted carbon becomes planar in the cation. These geometry changes enable each ground-state vibrational level to access a large number of vibrational levels within each Rydberg state. As a result, CHF_2 and CF_2CH_3 exhibit 3p Rydberg spectra that span nearly $\sim$11 000 cm^{-1}. The REMPI spectrum of CHF_2 is a distinct and well-resolved set of $\sim$85 vibrational bands. In contrast, the vibrational bands of CF_2CH_3 overlap into a continuum, and only one progression is partially resolved. The more congested spectrum exhibited by CF_2CH_3 reflects the greater density of accessible states within its vibrational manifold.

In contrast to the analyses of halomethyl radical spectra, analyses of haloethyl radical spectra must consider effects from isomerization processes. *Ab initio* calculations predict that isomerization does not affect the spectrum of CF_2CH_3 radicals. However, *ab initio* calculations do predict that $CHF_2CH_2^+$ isomerizes into $CF_2CH_3^+$. This isomerization will cause the CHF_2CH_2 isomer to produce broad continuous Rydberg spectra. The band system from each Rydberg state will be displaced well to the blue of each origin. The absence of vibrational features will complicate attempts to unambiguously assign each REMPI spectrum. In short, we expect that complications associated with the geometry changes, a high density of states, and isomerization will impede detailed investigations of the Rydberg spectra of many haloethyl radicals.

Acknowledgment. We thank Karl K. Irikura for advice regarding the *ab initio* calculations and for suggesting the method used to predict vibrational activity from *ab initio* results.

References and Notes

(1) Atkinson, R.; Baulch, D. L.; Cox, R. A.; Hampson, Jr., R. F.; Kerr, J. A.; Troe, J. *J. Phys. Chem. Ref. Data* **1992**, *21*, 1125.

(2) Johnson III, R. D.; Tsai, B. P.; Hudgens, J. W. *J. Chem. Phys.* **1989**, *91*, 4558.

(3) Certain commericial materials and equipment are identified in this paper in order to adequately specify the experimental procedure. In no case does such an identification imply recommendation or endorsement by the National Institute of Standards and Technology, nor does it imply that the material or equipment is necessarily the best available for the purpose.

(4) GAUSSIAN 92, Revision A: Frisch, M. J.; Trucks, G. W.; Head-Gordon, M.; Gill, P. M. W.; Wong, M. W.; Foresman, J. B.; Johnson, B. G.; Schlegel, H. B.; Robb, M. A.; Replogle, E. S.; Gomperts, R.; Andres, J. L.; Raghavachari, K.; Binkley, J. S.; Gonzalez, C.; Martin, R. L.; Fox, D. J.; Defrees, D. J.; Baker, J.; Stewart, J. J. P.; Pople, J. A. Gaussian, Inc., Pittsburgh, PA, 1992.

(5) Pople, J. A.; Head-Gordon, M.; Fox, D. J.; Raghavachari, K.; Curtiss, L. A. *J. Chem. Phys.* **1989**, *90*, 5622.

(6) Hudgens, J. W. In *Advances in Multi-photon Processes and Spectroscopy*; Lin, S. H., Ed.; World Scientific Publishing, Singapore, 1988; Vol. 4, pp 171–296.

(7) Hudgens, J. W.; Dulcey, C. S.; Long, G. R.; Bogan, D. J. *J. Chem. Phys.* **1987**, *87*, 4546.

(8) Tsai, B. P.; Johnson III, R. D.; Hudgens, J. W. *J. Phys. Chem.* **1989**, *93*, 5334.

(9) Hudgens, J. W.; Johnson III, R. D.; Tsai, B. P.; Kafafi, S. *J. Am. Chem. Soc.* **1990**, *112*, 5763.

(10) Kafafi, S.; Hudgens, J. W. *J. Phys. Chem.* **1989**, *93*, 3474.

(11) Dearden, D. V.; Hudgens, J. W.; Johnson III, R. D.; Tsai, B. P.; Kafafi, S. *J. Phys. Chem.* **1992**, *96*, 585.

(12) Hudgens, J. W.; Johnson III, R. D.; Tsai, B. P. *J. Chem. Phys.* **1993**, *98*, 1925.

(13) Brum, J.; Johnson III, R. D.; Hudgens, J. W. *J. Chem. Phys.* **1993**, *98*, 3732.

(14) Geometry-optimized MP2/6-31G* calculations for $CHFCH_2F^+$ obtained the total energy of −276.582 004 1 hartrees. The total energy of $CHFCH_2F^+$ is 1.45 eV higher than $CF_2CH_3^+$.

(15) Johnson III, R. D.; Brum, J. L. Manuscript in preparation.

(16) Chen, Y.; Rauk, A.; Tschuikow-Roux, E. *J. Chem. Phys.* **1990**, *93*, 1187.

(17) Lias, S. G.; Bartmess, J. E.; Liebman, J. F.; Holmes, J. L.; Levin, R. D.; Mallard, W. G. Gas-Phase Ion and Neutral Thermochemistry. *J. Phys. Chem. Ref. Data* **1988**, *17* (Suppl. No. 1). This reference lists $\Delta_f H_{298}^\circ$ = 452 kJ/mol. We obtain $\Delta_f H_0^\circ$ = 442 kJ/mol using the *ab initio* vibrational frequencies and rotational moments of inertia.

(18) Hehre, W. J.; Radom, L.; Schleyer, P. v. R.; Pople, J. A. *Ab Initio Molecular Orbital Theory*; J. Wiley & Sons: New York, 1986.

(19) Hudgens, J. W.; DiGiuseppe, T. G.; Lin, M. C. *J. Chem. Phys.* **1983**, *79*, 571–582.

(20) Johnson III, R. D.; Hudgens, J. W. *J. Phys. Chem.* **1987**, *91*, 6189.

(21) Dulcey, C. S.; Hudgens, J. W. *J. Chem. Phys.* **1986**, *84*, 5262.

(22) Irikura, K. K.; Johnson III, R. D.; Hudgens, J. W. *J. Phys. Chem.* **1992**, *96*, 6131.

(23) Johnson III, R. D. *J. Chem. Phys.* **1992**, *96*, 4073.